Combined Bound Tightening on McCormick Relaxations of AC Optimal Power Flow

Xiangxin An*, Constance Crozier*, Santanu S. Dey*, Santiago Grijalva†
*School of Industrial and Systems Engineering, †School of Electrical and Computer Engineering
Georgia Institute of Technology
Atlanta, GA 30332, USA
{xan45, constance, sdey30, sgrijalva6}@gatech.edu

***Abstract*—This paper investigates the effectiveness of combining valid inequalities and feasibility-based bound tightening (FBBT) to strengthen linear programming (LP) relaxations for the AC Optimal Power Flow (ACOPF) problem. We focus on reformulations using McCormick envelopes applied to the Second-Order Conic Programming (SOCP) relaxation of ACOPF. Several classes of valid inequalities, including ring cuts, reverse cone envelopes, and arctangent envelopes, are integrated into the relaxation. A combined tightening framework is proposed, beginning with bound tightening via SOCP relaxations, followed by adding valid inequalities and successive refinement of the McCormick envelopes with FBBT. Experimental results show that integrating arctangent envelopes with FBBT yields a tighter and more scalable relaxation. This approach significantly reduces the average SOCP gap from 8.14% to 4.11%, thereby improving the practical performance of convex relaxations for ACOPF.**

***Index Terms*—ACOPF, convex relaxation, bound tightening**

I. Introduction

The Alternating Current Optimal Power Flow (ACOPF) problem is fundamental in the operation of electric power grids, aiming at optimizing power generation and transmission while respecting the physical and operational constraints of the power network. However, due to the inherent physical nature of alternating power flow equations, ACOPF is nonlinear, nonconvex, and generally NP-Hard [1]. This combination of features brings significant challenges in solving ACOPF for large-scale power systems in real life.

To address the complexity of ACOPF, two main approaches are commonly used. The first approach involves approximating AC power flow with Direct Current (DC) power flow equations. This approximation linearizes the power flow equation by ignoring reactive power flow and voltage magnitude at the cost of lost accuracy of AC feasibility [2]. Additionally, various studies have proposed linear programming techniques to approximate AC power flow equations directly [3]–[6].

The second approach employs nonlinear solvers to find a local optimum. Methods such as the Newton-Raphson technique and interior-point algorithms are commonly used [7]. These methods are computationally feasible for medium-sized systems and can efficiently handle practical network configurations. However, they do not guarantee global optimality, which may lead to a significant gap between the local optimum obtained and the theoretical global solution.

To evaluate the quality of local optima, convex relaxations are used to derive lower bounds for ACOPF [8]. These relaxations reformulate the nonconvex problem into a convex one, enabling the use of efficient solvers while providing global optima as meaningful lower bounds on the original problem. Numerous studies have investigated reformulations and convex relaxation techniques, aiming to improve the accuracy and computational efficiency of these methods [7]. Currently, the most common convex relaxations for ACOPF include Semi-definite Programming (SDP) [9], Second-Order Conic Programming (SOCP) [10], Quadratic Convex Quadratic Programming (QC) [11] and Linear Programming (LP) [12]. SDP was proved to give a globally optimal solution on a number of tested ACOPF cases [13]. However, it is computationally demanding for large-scale problems. SOCP relaxations strike a balance between computational efficiency and accuracy but produce weaker bounds compared to SDP. QC relaxations offer an intermediate complexity with tighter bounds than LP but are still expensive to solve. LP relaxations, while computationally efficient, typically yield the loosest bounds and require additional techniques to be practically useful.

To further improve the tightness of convex relaxations of ACOPF, researchers have explored techniques such as adding valid inequalities and performing bound tightening on current convex relaxations, especially on the SOCP relaxation. For instance, Kocuk et al. [10] generated valid inequalities for the arctangent envelope, and projected the SDP relaxation over cycles to strengthen the SOCP relaxation. Similarly, Narimani et al. [14] used linear convex envelopes to tighten the QC relaxation. And Coffrin et al. [15] used lifted nonlinear cuts and feasibility-based bound tightening (FBBT) techniques to strengthen current SDP relaxations, which were first proposed in earlier works [16], [17]. These strategies help to reduce the gap between the relaxed feasible region and the original ACOPF solution space.

Despite these advancements, there remains a considerable gap between the potential of LP relaxation in theory and its practical performance in solving ACOPF. The main goal of this paper is to use combined valid inequalities and bound

This work was supported in part by the U.S. Department of Energy (DOE), Office of Energy Efficiency and Renewable Energy (EERE), Solar Energy Technologies Office (SETO) OPTIMA Program, under Award No. DE-EE0011376 to the Georgia Tech Research Corporation: ENVELOPE: Energy Variability and Electricity Optimization Using Stochastic Operational Envelopes.

tightening techniques to enhance the LP relaxation of ACOPF. By systematically integrating these techniques, we aim to reduce the gap between LP relaxation and the original feasible region while maintaining computational tractability.

II. Problem Formulations

In this section, we present the standard SOCP relaxation and the corresponding LP relaxation formulations for ACOPF. We begin by introducing the system model and relevant notations.

A. Branch-flow Model

Consider a transmission-level power network $\mathcal{N} = (\mathcal{B}, \mathcal{L})$, where $\mathcal{B}$ is the set of buses and $\mathcal{L}$ is the set of transmission lines. The set of generators is denoted by $\mathcal{G}$, and $\mathcal{G}_i \subseteq \mathcal{G}$ denotes the subset of generators located at bus i. For each generator k at bus i, the active and reactive power generation are denoted as p_k^g, q_k^g respectively, and the generation cost function, $C_k^g(p_k^g)$, for each generator k is usually linear or convex quadratic in p_k^g.

For each transmission line $\ell \in \mathcal{L}$ connecting buses i and j, we denote the line by tuple (ℓ, i, j). The sets of incoming and outgoing lines at bus i are given by $\delta^{in}(i) := \{\ell | (\ell, j, i) \in \mathcal{L}\}$ and $\delta^{out}(i) := \{\ell | (\ell, i, j) \in \mathcal{L}\}$, respectively. The physical parameters of each line ℓ are captured by its admittance matrix in complex form:

$$Y_{(\ell,i,j)} := \begin{pmatrix} G_\ell^{ff} + \mathrm{j}B_\ell^{ff} & G_\ell^{ft} + \mathrm{j}B_\ell^{ft} \\ G_\ell^{tf} + \mathrm{j}B_\ell^{tf} & G_\ell^{tt} + \mathrm{j}B_\ell^{tt} \end{pmatrix}$$

where G_ℓ^{ab} and B_ℓ^{ab} represent the conductance and susceptance of line ℓ from terminal a to b, with f and t indicating the line's *from* (bus i) and *to* (bus j) ends. At each bus i, let g_i^{sh} (resp. b_i^{sh}) denote the shunt conductance (resp. susceptance), the complex voltage at bus i can be represented in polar form as $V_i = |V_i|(\cos\theta_i + \mathrm{j}\sin\theta_i)$, where $|V_i|$ is the voltage magnitude and θ_i is the voltage angle. At the same time, the active and reactive power demand at bus i are denoted by p_i^d, q_i^d, where $p_i^d \geq 0$, $-\infty \leq q_i^d \leq \infty$. The polar form of the branch-flow model for ACOPF is described in (1)-(11).

$$\min_{p_k^g} \sum_{k \in \mathcal{G}} C_k^g(p_k^g) \tag{1}$$

$\forall$ transmission line $(\ell, i, j) \in \mathcal{L}$:

$$p_\ell^{ft} = G_\ell^{ff}|V_i|^2 + |V_i||V_j|(G_\ell^{ft}\cos\theta_{ij} + B_\ell^{ft}\sin\theta_{ij}) \tag{2}$$

$$q_\ell^{ft} = -B_\ell^{ff}|V_i|^2 - |V_i||V_j|(B_\ell^{ft}\cos\theta_{ij} - G_\ell^{ft}\sin\theta_{ij}) \tag{3}$$

$$p_\ell^{tf} = G_\ell^{tt}|V_j|^2 + |V_i||V_j|(G_\ell^{tf}\cos\theta_{ij} - B_\ell^{tf}\sin\theta_{ij}) \tag{4}$$

$$q_\ell^{tf} = -B_\ell^{tt}|V_i|^2 - |V_i||V_j|(B_\ell^{tf}\cos\theta_{ij} + G_\ell^{tf}\sin\theta_{ij}) \tag{5}$$

$\forall$ bus $i \in \mathcal{B}$:

$$\sum_{k \in \mathcal{G}_i} p_k^g - p_i^d = g_i^{sh}|V_i|^2 + \sum_{\ell \in \delta^{in}(i)} p_\ell^{ft} + \sum_{\ell \in \delta^{out}(i)} p_\ell^{tf} \tag{6}$$

$$\sum_{k \in \mathcal{G}_i} q_k^g - q_i^d = -b_i^{sh}|V_i|^2 + \sum_{\ell \in \delta^{in}(i)} q_\ell^{ft} + \sum_{\ell \in \delta^{out}(i)} q_\ell^{tf} \tag{7}$$

$$\forall \text{ generator } k \in \mathcal{G} : \underline{p}_i^g \leq p_i^g \leq \overline{p}_i^g, \underline{q}_i^g \leq q_i^g \leq \overline{q}_i^g \tag{8}$$

$$\forall \text{ bus } i \in \mathcal{B} : \underline{V}_i \leq |V_i| \leq \overline{V}_i \tag{9}$$

$\forall$ transmission line $(\ell, i, j) \in \mathcal{L}$:

$$(p_\ell^{ft})^2 + (q_\ell^{ft})^2 \leq \overline{S}_\ell^2, (p_\ell^{tf})^2 + (q_\ell^{tf})^2 \leq \overline{S}_\ell^2 \tag{10}$$

$$\underline{\theta}_\ell \leq \theta_{ij} \leq \overline{\theta}_\ell, \theta_{ij} = \theta_i - \theta_j \tag{11}$$

The objective function (1) minimizes the total generation cost across all generators. Constraints (2)-(5) describe the active and reactive power flows between the "from" and "to" buses of each transmission line ℓ. Power balance at each bus is enforced by (6) and (7). And the limits on active and reactive power generation are represented by (8). Voltage magnitude bounds at each bus i are imposed by (9). Finally, each transmission line ℓ is subject to thermal limits and phase angle difference constraints, specified in (10) and (11), respectively.

B. Jabr Relaxation

The classical SOCP relaxation for the ACOPF problem was first introduced by Jabr [18]. Following a similar reformulation, we define the auxiliary variables for each bus i and transmission line (i, j) as $c_{ii} = |V_i|^2$, $c_{ij} = |V_i||V_j|\cos\theta_{ij}$, $s_{ij} = -|V_i||V_j|\sin\theta_{ij}$. Using these variables, the power flow equations can be reformulated as shown in (12)-(15). The $|V_i|^2$ term in (6)(7) can be replaced by c_{ii}, and the voltage magnitude constraints are similarly transformed into (16). Based on the definitions of the new variables, we also derive the nonlinear constraint (17) and the angle difference constraint (18).

$\forall$ transmission line $(\ell, i, j) \in \mathcal{L}$:

$$p_\ell^{ft} = G_\ell^{ff}\, c_{ii} + G_\ell^{ft}\, c_{ij} - B_\ell^{ft}\, s_{ij} \tag{12}$$

$$q_\ell^{ft} = -B_\ell^{ff}\, c_{ii} - B_\ell^{ft}\, c_{ij} - G_\ell^{ft}\, s_{ij} \tag{13}$$

$$p_\ell^{tf} = G_\ell^{tt}\, c_{jj} + G_\ell^{tf}\, c_{ij} + B_\ell^{tf}\, s_{ij} \tag{14}$$

$$q_\ell^{tf} = -B_\ell^{tt}\, c_{jj} - B_\ell^{tf}\, c_{ij} + G_\ell^{tf}\, s_{ij} \tag{15}$$

$$\underline{V}_i^2 \leq c_{ii} \leq \overline{V}_i^2, i \in \mathcal{B} \tag{16}$$

$$c_{ij}^2 + s_{ij}^2 = c_{ii}\, c_{jj} \tag{17}$$

$$\theta_j - \theta_i = \arctan(s_{ij}/c_{ij}) \tag{18}$$

Since constraint (17) is non-convex, we relax it to be:

$$c_{ij}^2 + s_{ij}^2 \leq c_{ii}c_{jj}, \forall (\ell, i, j) \in \mathcal{L} \tag{19}$$

Therefore, the SOCP relaxation for ACOPF involves (1), modified (6) and (7), (8), (10), (12)-(16), and (19).

C. McCormick Relaxation

McCormick relaxations are broadly used in constructing LP relaxations for problems involving bilinear/quadratic terms [19]. Generally, the McCormick envelope provides a convex relaxation of a nonlinear nonconvex program by leveraging the known bounds of the variables. Specifically, for a bilinear term $w = xy$, where $\underline{x} \leq x \leq \overline{x}, \underline{y} \leq y \leq \overline{y}$, the McCormick relaxation is given by the following 4 linear inequalities (20)-(21), which define the tightest convex hull of w over the given box constraints:

$$w \geq x\underline{y} + \underline{x}y - \underline{x}\underline{y}, \qquad w \geq \overline{x}y + x\overline{y} - \overline{x}\overline{y} \tag{20}$$

$$w \leq x\overline{y} + \underline{x}y - \underline{x}\overline{y}, \qquad w \leq x\underline{y} + \overline{x}y - \overline{x}\underline{y} \tag{21}$$

To simplify notation, we denote the McCormick envelope of a bilinear term $w = xy$ as $M(w = xy)$. In constructing the McCormick relaxation for the ACOPF problem, we introduce auxiliary variables C_{ij}, D_{ij}, S_{ij}, P_ℓ^{ft},Q_ℓ^{ft}, P_ℓ^{tf}, and Q_ℓ^{tf} to replace the bilinear and quadratic terms appearing in constraints (10) and (17), reformulating these 2 constraints into linear expressions:

$$P_\ell^{ft} + Q_\ell^{ft} \leq \overline{S}_\ell^2, P_\ell^{tf} + Q_\ell^{tf} \leq \overline{S}_\ell^2, \quad \forall(\ell, i, j) \in \mathcal{L} \quad (22)$$
$$C_{ij} + S_{ij} = D_{ij}, \quad \forall(\ell, i, j) \in \mathcal{L} \quad (23)$$

Accordingly, the corresponding McCormick envelopes for each of these terms are then added, linearizing the model while preserving convexity within the bounds of the original variables.

$$M(C_{ij} = c_{ij}^2), M(S_{ij} = s_{ij}^2), M(D_{ij} = c_{ii}c_{jj}) \quad (24)$$
$$M(P_\ell^{ft} = (p_\ell^{ft})^2), M(Q_\ell^{ft} = (q_\ell^{ft})^2) \quad (25)$$
$$M(P_\ell^{tf} = (p_\ell^{tf})^2), M(Q_\ell^{tf} = (q_\ell^{tf})^2) \quad (26)$$

As a result, the final McCormick relaxation for the ACOPF problem retains the original objective function (1) and linear constraints (6)-(8) while replacing all bilinear and quadratic terms with their corresponding linear relaxations (12)-(16) and (22)-(26).

III. Tightening Techniques

This section outlines the main tightening techniques employed in this work, including valid inequalities and bound tightening strategies.

A. Valid Inequalities

We investigate three classes of valid inequalities to enhance the strength of the relaxation.

1) Ring Cuts: The idea of ring cuts originates from [20]. In this work, we extend the formulation to incorporate both the inner and outer boundaries of the ring region. Recall that the variables $c_{ij} = |V_i||V_j|\cos\theta_{ij}$ and $s_{ij} = -|V_i||V_j|\sin\theta_{ij}$ represent the real and imaginary parts of the voltage product between buses i and j. Naturally, these variables are constrained to lie within an annular region defined by:

$$\mathcal{R}_{ij} := \{(c_{ij}, s_{ij}) : \underline{R}_{ij}^2 \leq c_{ij}^2 + s_{ij}^2 \leq \overline{R}_{ij}^2\},$$

where $\underline{R}_{ij} = \underline{V}_i\underline{V}_j$, $\overline{R}_{ij} = \overline{V}_i\overline{V}_j$ are derived from the lower and upper bounds on the voltage magnitudes at buses i and j.

Based on the definitions of c_{ij}, s_{ij}, their initial bounds can be computed as:

$$\underline{c}_{ij} = \underline{V}_i\underline{V}_j\cos\underline{\theta}_{ij}, \qquad \overline{c}_{ij} = \overline{V}_i\overline{V}_j$$
$$\underline{s}_{ij} = -\overline{V}_i\overline{V}_j\sin\overline{\theta}_{ij}, \qquad \overline{s}_{ij} = -\overline{V}_i\overline{V}_j\sin\underline{\theta}_{ij}$$

These bounds define a rectangular region, whose intersection with the annular feasible set can be leveraged to construct valid inequalities - namely, ring cuts - that exclude infeasible regions while preserving all feasible solutions. We define the bounding box:

$$\mathcal{B}_{ij} := [\underline{c}_{ij}, \overline{c}_{ij}] \times [\underline{s}_{ij}, \overline{s}_{ij}],$$

which represents the initial relaxation region based on the variable bounds. The feasible region for (c_{ij}, s_{ij}) in the ACOPF problem is given by the intersection $\mathcal{R}_{ij} \cap \mathcal{B}_{ij}$.

Since $\underline{c}_{ij} \geq 0$, by analyzing the geometric relationship between the ring and the box, we can generate valid inequalities that cut off parts of $\mathcal{B}_{ij}$. In particular, when $\underline{c}_{ij} < \underline{R}_{ij}$, the inner boundary of the ring intersects with the box, resulting in up to three pairs of possible intersection points.

- $||(\underline{c}_{ij}, \underline{s}_{ij})|| < \underline{R}_{ij}$ and $||(\underline{c}_{ij}, \overline{s}_{ij})|| < \underline{R}_{ij}$: $x_1 = \sqrt{\underline{R}_{ij}^2 - \overline{s}_{ij}^2}$, $y_1 = \overline{s}_{ij}$; $x_2 = \sqrt{\underline{R}_{ij}^2 - \underline{s}_{ij}^2}$, $y_2 = \underline{s}_{ij}$
- $||(\underline{c}_{ij}, \underline{s}_{ij})|| < \underline{R}_{ij}$ and $||(\underline{c}_{ij}, \overline{s}_{ij})|| \geq \underline{R}_{ij}$: $x_1 = \underline{c}_{ij}$, $y_2 = \underline{s}_{ij}$, $y_1 = \sqrt{\underline{R}_{ij}^2 - \underline{c}_{ij}^2}$, $x_2 = \sqrt{\underline{R}_{ij}^2 - \underline{s}_{ij}^2}$
- $||(\underline{c}_{ij}, \underline{s}_{ij})|| \geq \underline{R}_{ij}$ and $||(\underline{c}_{ij}, \overline{s}_{ij})|| < \underline{R}_{ij}$: $y_1 = \overline{s}_{ij}$, $x_2 = \underline{c}_{ij}$, $x_1 = \sqrt{\underline{R}_{ij}^2 - \overline{s}_{ij}^2}$, $y_2 = -\sqrt{\underline{R}_{ij}^2 - \underline{c}_{ij}^2}$

Based on this geometric configuration, we derive a valid inequality that excludes the infeasible interior region of the inner circle, represented by (27):

$$(y_1 - y_2)c_{ij} - (x_1 - x_2)s_{ij} \geq x_2y_1 - x_1y_2. \quad (27)$$

For the outer boundary of the ring, the intersection between $\mathcal{R}_{ij}$ and $\mathcal{B}_{ij}$ occurs under specific geometric configurations. These scenarios arise when parts of $\mathcal{B}_{ij}$ extend beyond the outer radius $\overline{R}_{ij}$, resulting in infeasible regions outside the permissible voltage product magnitudes:

- $||(\overline{c}_{ij}, \overline{s}_{ij})|| > \overline{R}_{ij}$ and $||(\overline{c}_{ij}, \underline{s}_{ij})|| > \overline{R}_{ij}$: $y_1 = \overline{s}_{ij}$, $y_2 = \underline{s}_{ij}$, $x_1 = \sqrt{\overline{R}_{ij}^2 - \overline{s}_{ij}^2}$, $x_2 = \sqrt{\overline{R}_{ij}^2 - \underline{s}_{ij}^2}$.
- $||(\overline{c}_{ij}, \overline{s}_{ij})|| \leq \overline{R}_{ij}$ and $||(\overline{c}_{ij}, \underline{s}_{ij})|| > \overline{R}_{ij}$: $x_1 = \overline{c}_{ij}$, $y_2 = \underline{s}_{ij}$, $y_1 = -\sqrt{\overline{R}_{ij}^2 - \overline{c}_{ij}^2}$, $x_2 = \sqrt{\overline{R}_{ij}^2 - \underline{s}_{ij}^2}$.
- $||(\overline{c}_{ij}, \overline{s}_{ij})|| > \overline{R}_{ij}$ and $||(\overline{c}_{ij}, \underline{s}_{ij})|| \leq \overline{R}_{ij}$: $y_1 = \overline{s}_{ij}$, $x_2 = \overline{c}_{ij}$, $x_1 = \sqrt{\overline{R}_{ij}^2 - \overline{s}_{ij}^2}$, $y_2 = \sqrt{\overline{R}_{ij}^2 - \overline{c}_{ij}^2}$.

In such cases, a valid inequality can be derived to exclude these infeasible portions. The resulting constraint, denoted as (28), ensures that the solution lies within or inside the outer circle, thereby preserving feasibility with respect to the physical model while tightening the relaxation.

$$(x_1 - x_2)s_{ij} \geq (y_1 - y_2)c_{ij} - \overline{R}_{ij}\sqrt{(x_1 - x_2)^2 + (y_1 - y_2)^2} \quad (28)$$

2) Arctangent Envelopes: Arctangent envelopes are used to construct outer linear approximations of the nonlinear constraints in the case of angular relationships (18). With the assumption that the phase angle difference is small enough [13], we have $c_{ij} > 0$. Following the approach in [10], we consider the set:

$$\mathcal{A}_{ij} := \{(c_{ij}, s_{ij}, \theta_{ji}) \in \mathbf{R}^3 : \theta_{ji} = \arctan(s_{ij}/c_{ij}),$$
$$(c_{ij}, s_{ij}) \in [\underline{c}_{ij}, \overline{c}_{ij}] \times [\underline{s}_{ij}, \overline{s}_{ij}]\},$$

where θ_{ji} denotes the angle difference $\theta_j - \theta_i$. To approximate $\mathcal{A}_{ij}$, we consider the convex hull of its graph over the specified box $\mathcal{B}_{ij}$. Project the four corner points of $\mathcal{B}_{ij}$ in 2D onto the arctangent surface

$\theta_{ji} = \arctan(s_{ij}/c_{ij})$, then we will get 4 corner points of $\mathcal{A}_{ij}$ in 3D: $z^1_{ij} = (\underline{c}_{ij}, \overline{s}_{ij}, \arctan(\overline{s}_{ij}/\underline{c}_{ij}))$, $z^2_{ij} = (\overline{c}_{ij}, \overline{s}_{ij}, \arctan(\overline{s}_{ij}/\overline{c}_{ij}))$, $z^3_{ij} = (\overline{c}_{ij}, \underline{s}_{ij}, \arctan(\underline{s}_{ij}/\overline{c}_{ij}))$, and $z^4_{ij} = (\underline{c}_{ij}, \underline{s}_{ij}, \arctan(\underline{s}_{ij}/\underline{c}_{ij}))$.

Two supporting planes that pass through the point triples $\{z^1_{ij}, z^2_{ij}, z^3_{ij}\}$ and $\{z^1_{ij}, z^3_{ij}, z^4_{ij}\}$ define the upper approximation of $\mathcal{A}$, denoted as $\theta^1_{ji} = \gamma_1 + \alpha_1 c_{ij} + \beta_1 s_{ij}$ and $\theta^2_{ji} = \gamma_2 + \alpha_2 c_{ij} + \beta_2 s_{ij}$. These yield two valid inequalities, collectively referred to as the upper envelopes of $\mathcal{A}$:

$$\begin{aligned} &\gamma'_k + \alpha_k c_{ij} + \beta_k s_{ij} \geq \theta_{ji}, \\ &\text{where } \gamma'_k = \gamma_k + \Delta\gamma_k, \\ &\Delta\gamma_k = \max_{(c_{ij}, s_{ij}) \in \mathcal{B}_{ij}} \{\arctan(s_{ij}/c_{ij}) - \theta^k_{ji}\}, \\ &\theta^k_{ji} = \gamma_k + \alpha_k c_{ij} + \beta_k s_{ij}, \text{and } k = 1, 2. \end{aligned} \tag{29}$$

Similarly, the lower envelope is constructed by fitting the planes $\theta^3_{ji} = \gamma_3 + \alpha_3 c_{ij} + \beta_3 s_{ij}$ and $\theta^4_{ji} = \gamma_4 + \alpha_4 c_{ij} + \beta_4 s_{ij}$ through the points triples $\{z^1_{ij}, z^2_{ij}, z^4_{ij}\}$ and $\{z^2_{ij}, z^3_{ij}, z^4_{ij}\}$, respectively. The valid inequalities that form the lower envelopes of $\mathcal{A}$ are:

$$\begin{aligned} &\gamma'_k + \alpha_k c_{ij} + \beta_k s_{ij} \leq \theta_{ji}, \\ &\text{where } \gamma'_k = \gamma_k - \Delta\gamma_k, \\ &\Delta\gamma_k = \max_{(c_{ij}, s_{ij}) \in \mathcal{B}_{ij}} \{\theta^k_{ji} - \arctan(s_{ij}/c_{ij})\}, \\ &\theta^k_{ji} = \gamma_k + \alpha_k c_{ij} + \beta_k s_{ij}, \text{and } k = 3, 4. \end{aligned} \tag{30}$$

3) Reverse Cone Envelopes: The original relationship between c_{ij} and s_{ij} is given by (17), which can be expressed as $c_{ii}c_{jj} \leq c^2_{ij} + s^2_{ij} \leq c_{ii}c_{jj}$. However, the left-hand side inequality, $c_{ii}c_{jj} \leq c^2_{ij} + s^2_{ij}$, is non-convex and defines a reverse second-order cone. To approximate this non-convex region, we follow the approach in [21], constructing an outer approximation by overestimating $\sqrt{c^2_{ij} + s^2_{ij}}$ and underestimating $\sqrt{c_{ii}c_{jj}}$ using affine hyperplanes.

Specifically, we introduce affine functions $g^m(c_{ii}, c_{jj}) := \eta^m_{ij} c_{ii} + \zeta^m_{ij} c_{jj} + \kappa^m_{ij}$, $m = 1, 2$, which serve as underestimators of $\sqrt{c_{ii}c_{jj}}$ over the bounding box $\mathcal{B}_{ij}$.

$$\begin{aligned} \eta^1_{ij} &= \frac{\sqrt{\underline{c}_{jj}}}{\sqrt{\underline{c}_{ii}} + \sqrt{\overline{c}_{ii}}}, \eta^2_{ij} = \frac{\sqrt{\overline{c}_{jj}}}{\sqrt{\underline{c}_{ii}} + \sqrt{\overline{c}_{ii}}}, \\ \zeta^1_{ij} &= \frac{\sqrt{\underline{c}_{ii}}}{\sqrt{\underline{c}_{jj}} + \sqrt{\overline{c}_{jj}}}, \zeta^2_{ij} = \frac{\sqrt{\overline{c}_{ii}}}{\sqrt{\underline{c}_{jj}} + \sqrt{\overline{c}_{jj}}}, \\ \kappa^1_{ij} &= \sqrt{\underline{c}_{ii}\underline{c}_{jj}} - \eta^1_{ij}\underline{c}_{ii} - \zeta^1_{ij}\underline{c}_{jj}, \\ \kappa^2_{ij} &= \sqrt{\overline{c}_{ii}\overline{c}_{jj}} - \eta^2_{ij}\overline{c}_{ii} - \zeta^2_{ij}\overline{c}_{jj}. \end{aligned}$$

Similarly, the affine functions $f^n(c_{ij}, s_{ij}) := \eta^n_{ij} c_{ij} + \zeta^n_{ij} s_{ij} + \kappa^n_{ij}$, $n = 3, 4$ provide overestimations of $\sqrt{c^2_{ij} + s^2_{ij}}$ over the same domain.

$$\Omega := \sqrt{\overline{c}^2_{ij} + \overline{s}^2_{ij}} + \sqrt{\underline{c}^2_{ij} + \underline{s}^2_{ij}} - \sqrt{\overline{c}^2_{ij} + \underline{s}^2_{ij}} - \sqrt{\underline{c}^2_{ij} + \overline{s}^2_{ij}}$$

$$\omega := \frac{\sqrt{\overline{c}^2_{ij} + \underline{s}^2_{ij}} - \sqrt{\underline{c}^2_{ij} + \underline{s}^2_{ij}}}{\overline{c}_{ij} - \underline{c}_{ij}}, \omega' := \frac{\sqrt{\overline{c}^2_{ij} + \overline{s}^2_{ij}} - \sqrt{\underline{c}^2_{ij} + \overline{s}^2_{ij}}}{\overline{c}_{ij} - \underline{c}_{ij}}$$

$$\eta^3_{ij} = \begin{cases} \omega, & \Omega < 0 \\ \omega', & \text{otherwise} \end{cases}, \eta^4_{ij} = \begin{cases} \omega', & \Omega < 0 \\ \omega, & \text{otherwise} \end{cases}$$

$$\zeta^3_{ij} = \frac{\sqrt{\underline{c}^2_{ij} + \overline{s}^2_{ij}} - \sqrt{\underline{c}^2_{ij} + \underline{s}^2_{ij}}}{\overline{s}_{ij} - \underline{s}_{ij}}, \zeta^4_{ij} = \frac{\sqrt{\overline{c}^2_{ij} + \overline{s}^2_{ij}} - \sqrt{\overline{c}^2_{ij} + \underline{s}^2_{ij}}}{\overline{s}_{ij} - \underline{s}_{ij}},$$

$$\kappa^3_{ij} = \sqrt{\underline{c}^2_{ij} + \underline{s}^2_{ij}} - \eta^3_{ij}\underline{c}_{ij} - \zeta^3_{ij}\underline{s}_{ij},$$

$$\kappa^4_{ij} = \sqrt{\overline{c}^2_{ij} + \overline{s}^2_{ij}} - \eta^4_{ij}\overline{c}_{ij} - \zeta^4_{ij}\overline{s}_{ij}.$$

The resulting valid inequalities, denoted in (31), form a convex outer approximation of the non-convex constraint $\sqrt{c_{ii}c_{jj}} \leq \sqrt{c^2_{ij} + s^2_{ij}}$:

$$\begin{aligned} &\eta^m_{ij} c_{ii} + \zeta^m_{ij} c_{jj} + \kappa^m_{ij} \leq \eta^n_{ij} c_{ij} + \zeta^n_{ij} s_{ij} + \kappa^n_{ij}, \\ &\text{where } m = 1, 2, \text{and } n = 3, 4. \end{aligned} \tag{31}$$

B. Bound Tightening

Bound tightening is a widely used technique for iteratively reducing the feasible ranges of variables, thereby strengthening convex relaxations. In [16], it was demonstrated that applying FBBT to the voltage magnitude and angle variables in the polar formulation significantly improves the performance of SDP and QC relaxations. Further work in [15] applied similar techniques to the QC relaxation, including objective-based bound tightening. In addition, [17] explored bound tightening on nodal power variables.

In this work, we extend these ideas by applying FBBT to the variables c_{ij} and s_{ij}, as used in the SOCP relaxation. Since the McCormick envelopes (24) depend directly on the bounds of these two variables, we update both the variable bounds and the corresponding McCormick envelopes at each iteration as new bounds are obtained. The complete procedure is detailed in Algorithm 1.

Algorithm 1 FBBT for c_{ij} and s_{ij}.

1: **Initialize:**
- Set $\underline{c}^0_{ij}, \overline{c}^0_{ij}, \underline{s}^0_{ij}, \overline{s}^0_{ij} := \underline{c}_{ij}, \overline{c}_{ij}, \underline{s}_{ij}, \overline{s}_{ij}$, max iter K;
- Set $\mathcal{S}$:= McCormick relaxation of ACOPF;
- Set iteration counter $k := 1$.

2: **repeat**
3: **for all** $c_{ij}, s_{ij}, (\ell, i, j) \in \mathcal{L}$: **do**
4: Calculate $\underline{c}'_{ij} := \min c_{ij} \in \mathcal{S}$, $\overline{c}'_{ij} := \max c_{ij} \in \mathcal{S}$; $\underline{s}'_{ij} := \min s_{ij} \in \mathcal{S}$, $\overline{s}'_{ij} := \max s_{ij} \in \mathcal{S}$;
5: Set $\underline{c}^k_{ij} := \max\{\underline{c}'_{ij}, \underline{c}^{k-1}_{ij}\}$, $\overline{c}^k_{ij} := \min\{\overline{c}'_{ij}, \overline{c}^{k-1}_{ij}\}$, $\underline{s}^k_{ij} := \max\{\underline{s}'_{ij}, \underline{s}^{k-1}_{ij}\}$, $\overline{s}^k_{ij} := \min\{\overline{s}'_{ij}, \overline{s}^{k-1}_{ij}\}$.
6: Update $\mathcal{S}$ with bounds $\underline{c}^k_{ij}, \overline{c}^k_{ij}, \underline{s}^k_{ij}, \overline{s}^k_{ij}$ and new McCormick envelopes of (24).
7: **end for**
8: $k \leftarrow k + 1$.
9: **until** $\underline{c}^k_{ij}, \overline{c}^k_{ij}, \underline{s}^k_{ij}, \overline{s}^k_{ij} = \underline{c}^{k-1}_{ij}, \overline{c}^{k-1}_{ij}, \underline{s}^{k-1}_{ij}, \overline{s}^{k-1}_{ij}$ or $k \geq K$.

C. Combined Tightening Framework

Our tightening framework combines valid inequalities and FBBT to evaluate the potential improvement in LP relaxations of the ACOPF problem.

The procedure begins by constructing two models, a standard SOCP relaxation and a McCormick relaxation, based on

the given instance parameters. Initial bounds on variables c_{ij} and s_{ij}, denoted $\underline{c}^0_{ij}$, $\overline{c}^0_{ij}$, $\underline{s}^0_{ij}$, $\overline{s}^0_{ij}$, are computed using the given limits on voltage magnitudes V_i, V_j and angle differences θ_{ij}.

At the first iteration, the SOCP relaxation is used to perform bound tightening on c_{ij} and s_{ij}, yielding new bounds $\underline{c}'_{ij}$, $\overline{c}'_{ij}$, $\underline{s}'_{ij}$, $\overline{s}'_{ij}$. New bounds are updated by selecting the most restrictive bounds: $\underline{c}^1_{ij} = \max\{\underline{c}^0_{ij}, \underline{c}'_{ij}\}$, $\overline{c}^1_{ij} = \min\{\overline{c}^0_{ij}, \overline{c}'_{ij}\}$; $\underline{s}^1_{ij} = \max\{\underline{s}^0_{ij}, \underline{s}'_{ij}\}$, $\overline{s}^1_{ij} = \min\{\overline{s}^0_{ij}, \overline{s}'_{ij}\}$.

At the second iteration, updated bounds are recomputed for each line using the current McCormick relaxation model. At this stage, additional valid inequalities (cuts) are introduced to further tighten the feasible region, and the McCormick envelopes are reconstructed accordingly.

For subsequent iterations ($k \geq 3$), the previously generated cuts are retained to ensure numerical stability. Only FBBT and McCormick envelope updates are performed in these iterations. The iterative procedure terminates when either a pre-specified maximum number of iterations is reached or when the bounds on all c_{ij} and s_{ij} remain unchanged relative to the previous iteration.

IV. Experimental Results

This section presents the experimental results. The test instances are drawn from the `PGLib-opf/api` library, v23.07 [22]. All experiments are conducted on a machine equipped with an Apple M3 processor and 16 GB of RAM, using the Julia 1.10 programming environment. IPOPT 1.10 is used to solve nonlinear programming (NLP) models, MOSEK 11.0 is used for SOCP, and GUROBI 12.0 is used to solve LP models.

A. Small instance analysis

We use the `pglib_opf_case3_lmbd__api` instance to illustrate the detailed procedure of our algorithm. Figure 1 illustrates the evolution of the bounds for each transmission line in this 3-bus system throughout iterations. Note that here we only add arctangent envelopes as the valid inequalities in the second iteration.

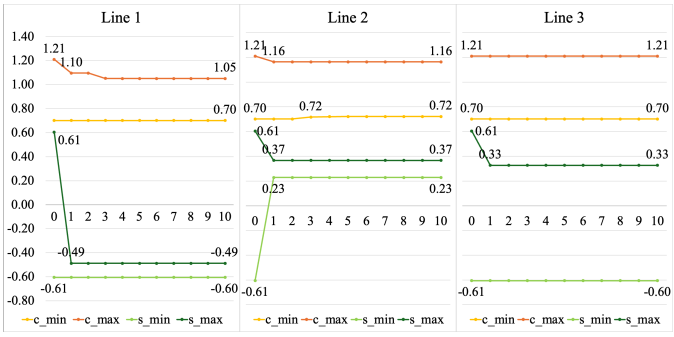

Fig. 1. Bounds of c, s variables on transmission lines for 10 rounds of combined bound tightening of a 3-bus system

From the iterative process, we observe that the most significant tightening of bounds occurs in the first iteration, driven by the SOCP relaxation. After the first iteration, the bounds continue to improve gradually over subsequent iterations. This additional tightening is attributed the effect of updating McCormick envelopes. While the magnitude of improvement diminishes with each iteration, the bounds converge steadily.

B. Performance of valid inequalities

To evaluate the effectiveness of different valid inequalities, we apply our iterative tightening framework while incorporating various types of valid inequalities beginning from the second iteration. The experiments are conducted on all `PGLib` benchmark instances with fewer than 500 buses.

Among a total of 19 test cases, 3 instances are infeasible during the bound tightening process and are therefore excluded from the analysis. For the remaining 16 feasible instances, we compute the optimality gap (`OptGap`) between the relaxation solution and the local optimum after each iteration. The local optimum (`LocalOpt`) for each instance is obtained by solving the ACOPF model in polar form. Figure 2 summarizes the average gap reduction achieved over the iterations for different types of valid inequalities, enabling a direct comparison of their impact on tightening the relaxation.

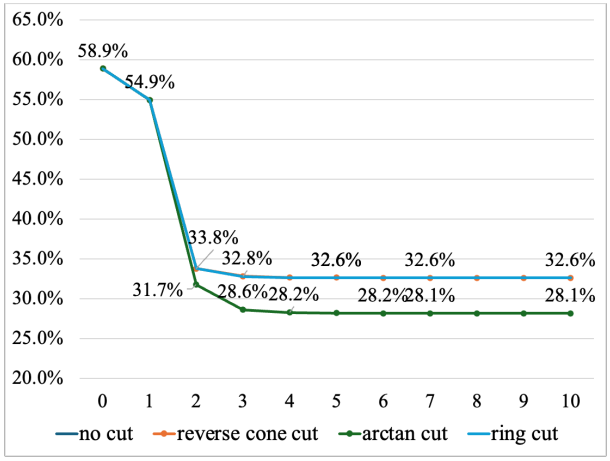

Fig. 2. Average optimality gap in 10 rounds of combined bound tightening with different valid inequalities

Figure 2 shows that the iterative tightening procedure converges within 4 to 6 iterations, after which the average optimality gap remains stable. When comparing the impact of different valid inequalities, we find that ring cuts and reverse cone cuts offer little improvement over the baseline with no cuts, with final gaps stabilizing at around 32.6%. In contrast, the arctangent envelope demonstrates a more substantial effect, reducing the average gap from 32.6% to 28.1%. This indicates that the arctangent cuts provide a significantly tighter relaxation. Therefore, in the following analysis, we keep the bound tightening with arctangent envelopes as our main algorithm.

C. Performance of bound tightening

Noticeable, the tightened bounds obtained from the McCormick relaxation can also be used to strengthen the original SOCP relaxation. To evaluate the effectiveness of valid inequalities and bound tightening, we compare the optimality gaps (`OptGap`) between various SOCP relaxations and the local optimum (`LocalOpt`). The baseline model, denoted

SOCP, corresponds to the model described in II-B. Building on this, SOCP_A augments the original model with arctangent envelopes derived using the initial bounds of c_{ij}, s_{ij}. SOCP_B incorporates the tightened bounds obtained after the bound tightening procedure, without additional valid inequalities. And SOCP_AB combines both enhancements by tightening the bounds and also applying arctangent envelopes using the updated bounds. The resulting gap comparisons are reported in Table I.

TABLE I
OPTIMALITY GAPS (%) OF SOCPS RELATIVE TO LOCAL OPTIMUM

Instance	SOCP	SOCP_A	SOCP_B	SOCP_AB
case3_lmbd	6.607%	6.426%	5.406%	4.186%
case5_pjm	1.746%	1.746%	1.746%	0.132%
case14_ieee	5.127%	5.127%	5.127%	2.516%
case24_ieee_rts	7.477%	7.477%	4.525%	0.755%
case30_as	44.601%	44.601%	44.558%	21.423%
case30_ieee	5.426%	5.426%	4.632%	1.052%
case39_epri	1.417%	1.417%	1.012%	0.325%
case57_ieee	8.197%	8.197%	7.244%	2.561%
case60_c	2.061%	2.061%	2.061%	1.662%
case73_ieee_rts	4.202%	4.202%	2.569%	0.894%
case118_ieee	26.165%	26.154%	26.154%	16.429%
case162_ieee_dtc	4.323%	4.321%	4.323%	4.255%
case179_goc	8.272%	8.186%	8.272%	5.795%
case200_activ	0.018%	0.018%	0.018%	0.011%
case300_ieee	0.944%	0.937%	0.944%	0.399%
case500_goc	3.647%	3.647%	3.609%	3.285%
Average	**8.139%**	**8.121%**	**7.637%**	**4.105%**

The average optimality gap between the original SOCP relaxation and the local optimum is 8.139%. Applying the arctangent envelopes using only the original bounds yields a tiny improvement, reducing the gap slightly to 8.121%. At the same time, applying bound tightening alone reduces the gap more noticeably, bringing it down to 7.637%. The most significant improvement is achieved through the combined application of bound tightening and strengthened arctangent envelopes, which together reduce the average gap to 4.105%.

In summary, the arctangent envelopes are the most effective among the tested valid inequalities. When combined with FBBT, they significantly enhance the quality of the convex relaxation, narrowing the gap to the local optimum and improving overall relaxation strength.

V. CONCLUSION

In this work, we proposed a tightening framework that integrates FBBT with various valid inequalities to improve LP relaxations of the ACOPF problem. Among the tested cuts, arctangent envelopes proved the most effective in reducing the optimality gap, consistently outperforming the baseline and other cut types, an observation also supported by [10]. When combined with bound tightening, this method consistently narrows the feasible region and strengthens the relaxation. Applying the resulting bounds and constraints back to the SOCP model further reduces the gap to the local optimum from 8.139% to 4.105%. Overall, these results demonstrate that integrating arctangent envelopes with bound tightening provides a powerful and effective approach for improving convex relaxations of the ACOPF problem.

REFERENCES

[1] D. Bienstock and A. Verma, "Strong NP-hardness of AC power flows feasibility," *Oper. Res. Lett.*, vol. 47, no. 6, pp. 494–501, 2019.

[2] K. Baker, "Solutions of DCOPF are never AC feasible," in *Proc. 12th ACM Int. Conf. Future Energy Syst.*, pp. 264–268, Jun. 2021.

[3] C. Coffrin and P. Van Hentenryck, "A linear-programming approximation of AC power flows," *INFORMS J. Comput.*, vol. 26, no. 4, pp. 718–734, May 2014.

[4] A. Castillo, P. Lipka, J. Watson, S. S. Oren, and R. P. O'Neill, "A successive linear programming approach to solving the IV-ACOPF," *IEEE Trans. Power Syst.*, vol. 31, no. 4, pp. 2752–2763, Jul. 2016.

[5] Z. Yang, H. Zhong, Q. Xia, A. Bose, and C. Kang, "Optimal power flow based on successive linear approximation of power flow equations," *IET Gener. Transm. Distrib.*, vol. 10, pp. 3654–3662, 2016.

[6] P. Fortenbacher and T. Demiray, "Linear/quadratic programming-based optimal power flow using linear power flow and absolute loss approximations," *Int. J. Electr. Power Energy Syst.*, vol. 107, pp. 680–689, May 2019.

[7] D. K. Molzahn and I. A. Hiskens, "A survey of relaxations and approximations of the power flow equations," *Found. Trends Electr. Energy Syst.*, vol. 4, no. 1/2, pp. 1–221, Feb. 2019.

[8] R. Madani, S. Sojoudi, and J. Lavaei, "Convex relaxation for optimal power flow problem: Mesh networks," *IEEE Trans. Power Syst.*, vol. 30, no. 1, pp. 199–211, Jan. 2015.

[9] X. Bai, H. Wei, K. Fujisawa, and Y. Wang, "Semidefinite programming for optimal power flow problems," *Int. J. Electr. Power Energy Syst.*, vol. 30, no. 6–7, pp. 383–392, 2008.

[10] B. Kocuk, S. S. Dey, and X. A. Sun, "Strong SOCP relaxations for the optimal power flow problem," *Oper. Res.*, vol. 64, no. 6, pp. 1177–1196, May 2016.

[11] H. Hijazi, C. Coffrin, and P. Van Hentenryck, "Convex quadratic relaxations of mixed-integer nonlinear programs in power systems," unpublished. [Online]. Available: http://www.optimization-online.org/DB_HTML/2013/09/4057.html

[12] D. Bienstock and M. Villagra, "Accurate and warm-startable linear cutting-plane relaxations for ACOPF," *arXiv preprint*, arXiv:2403.08800, Feb. 2024.

[13] R. Zimmerman, C. Murillo-Sánchez, and R. Thomas, "Matpower: Steady-state operations, planning, and analysis tools for power systems research and education," *IEEE Trans. Power Syst.*, vol. 26, no. 1, pp. 12–19, Feb. 2011.

[14] M. R. Narimani, D. K. Molzahn, K. R. Davis, and M. L. Crow, "Tightening QC relaxations of AC optimal power flow through improved linear convex envelopes," *IEEE Trans. Power Syst.*, vol. 40, no. 2, pp. 1465–1480, Mar. 2025.

[15] C. Coffrin, H. L. Hijazi, and P. Van Hentenryck, "Strengthening the SDP relaxation of AC power flows with convex envelopes, bound tightening, and valid inequalities," *IEEE Trans. Power Syst.*, vol. 32, no. 5, pp. 3549–3558, Sep. 2017.

[16] C. Coffrin, H. L. Hijazi, and P. Van Hentenryck, "Strengthening the SDP relaxation of AC power flows with convex envelopes, bound tightening, and lifted nonlinear cuts," *CoRR*, arXiv:1512.04644, 2015. [Online]. Available: http://arxiv.org/abs/1512.04644

[17] C. Chen, A. Atamtürk, and S. S. Oren, "Bound tightening for the alternating current optimal power flow problem," *IEEE Trans. Power Syst.*, vol. 31, no. 5, pp. 3729–3736, 2016.

[18] R. A. Jabr, "Radial distribution load flow using conic programming," *IEEE Trans. Power Syst.*, vol. 21, no. 3, pp. 1458–1459, Aug. 2006.

[19] G. P. McCormick, "Computability of global solutions to factorable nonconvex programs: Part I—Convex underestimating problems," *Math. Program.*, vol. 10, no. 1, pp. 147–175, 1976.

[20] B. Kocuk, S. S. Dey, and X. A. Sun, "Inexactness of SDP relaxation and valid inequalities for optimal power flow," *IEEE Trans. Power Syst.*, vol. 31, no. 1, pp. 642–651, Mar. 2016.

[21] B. Kocuk, S. S. Dey, and X. A. Sun, "Matrix minor reformulation and SOCP-based spatial branch-and-cut method for the AC optimal power flow problem," *Math. Program. Comput.*, vol. 10, no. 4, pp. 557–596, 2018.

[22] S. Babaeinejadsarookolaee *et al.*, "The power grid library for benchmarking AC optimal power flow algorithms," *arXiv preprint*, arXiv:1908.02788, Aug. 2019.